

Finite Element Application to Human Humerus Bone: A Biomechanical Study

Chetna Masih, Raji Nareliya and Veerendra Kumar

Abstract The purpose of this retrospective study is to evaluate the biomechanical behavior of the human humerus bone under specific boundary and loading conditions. The shape and material properties of the bones are based on the computed tomography (CT) data set, which was obtained from the Medical College, Jabalpur. Here, the Finite Element Analysis (FEA) which has an important significance in the biomechanical research has been used and its purpose in the field of biomechanics is to predict the mechanical behavior of bones; it is also a powerful computational tool that permits accurate structural analysis. Here, an analytical model of human humerus bone is developed to predict the stress and strain distribution developed. In the model, stress values increased with the increase of the axial load. The results of this analysis are helpful for orthopedic surgeons for clinical interest and bone prosthesis.

Keywords Biomechanical · Computed tomography · Finite element analysis · Humerus bone and prosthesis

V. Kumar

Government Engineering College, Jabalpur, India

e-mail: prof.veerendra.kumar@gmail.com

R. Nareliya

Hitkarni College of Engineering and Technology, Jabalpur, India

e-mail: raji_nareliya@yahoo.co.in

C. Masih (✉)

Government Engineering College, Gokhalpur, Jabalpur, MP 482 011, India

e-mail: chetnamasih@gmail.com

Introduction

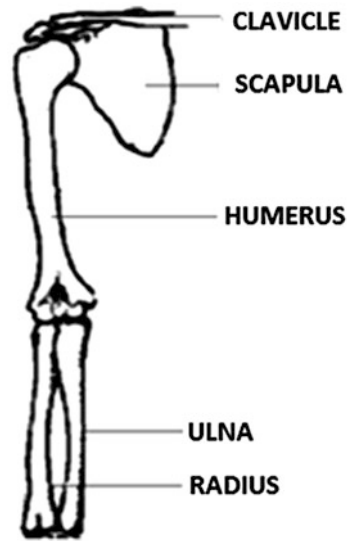
Anatomy of Humerus Bone

Humerus is the longest and the largest bone of the upper limb. It comprises a rounded head at the upper end, the shaft, and the expanded lower end. This bone pivots in three rotational degrees of freedom from its proximal end at the shoulder joint [1]. The head of the humerus forms less than half of the sphere and its smooth surface is covered by hyaline cartilage which articulates with the glenoid cavity with the scapula forming a ball and socket joint. It lies at an angle to the shaft and fits into a shallow socket of the scapula also known as shoulder blade to form the shoulder joint [2]. The anatomical neck is a slight constriction separating the head from the rest of the upper end of the humerus. The shaft is almost cylindrical in the upper half of its extent, prismatic and is flattened below [3]. It is not a weight bearing bone and therefore weight bearing is not a factor and shortening does not significantly worsen the end results. Humeral shaft fractures result from direct and indirect trauma. Pure compressive forces result in proximal and distal humerus fractures; bending forces, however, typically result in transverse fractures of the humerus shaft [4]. Humerus connects the shoulder by articulating the humeral head with the glenoid of the scapula, to the elbow by articulating the distal humerus with the ulna and radius, as shown in Fig. 1 [5]. The elbow is one of the few places in the body where two bones articulate with one bone [6].

Biomechanics of Bones

FE models of long bones constructed from CT data are an invaluable tool in the field of bone biomechanics. The structural properties of bone consist of the size, shape, and architecture of bones in addition to mechanical properties of bone tissue [7]. Bone tissue is a type of dense connective hard tissue. Bones are composed of inorganic salts impregnated in a matrix of collagen fibers, proteins, and minerals. They maintain the shape of the body and assist in force transmission during movement [8]. The mechanical properties of bone vary between species and individuals or due to age and disease [9]. Bone mass is increased by mechanical loading through the application of resistance or increased weight bearing activity [10]. One method to analyze the loading of the bone is by biomechanical modeling [11].

Fig. 1 Humerus bone in human arm



Adaption of Bone to Mechanical Loading

In loading, pure longitudinal, axial force such as compression slightly shortens and widens the bone while tension lengthens and narrows the bone. Bending mainly compresses the other side of the long bone and elongates the other. Bone is at its weakest at coping with the shear forces, better at coping with tension, and at its best for coping with compression [12]. Forces in habitual loading are most likely a combination of more than one, however, [13]. The anisotropic nature of bone reflects its function since bone structure is strongest in the primary loading condition [14].

Research Methodology

1. Obtain the sample data

The geometrical data of real proximal human humerus bone in the format of Digital Imaging and Communications in Medicine (DICOM) images of a 17-year-old male, whose weight is 75 kg, is obtained from CT scan data. A single DICOM file contains a header that stores information about the patient's names, the type of scan, image dimensions, and the image data, which contains information in three dimensions [15]. This DICOM data set is obtained from GE Signa HDXt 2008 Multi Channel 1.5 Tesla Superconducting Helium Cooled whole-body MR module machine and contains a total of 909 slices. This machine can perform with highest

Fig. 2 Yellow-colored mask of Humerus bone

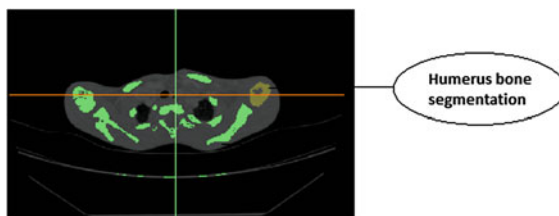


Fig. 3 Surface mesh

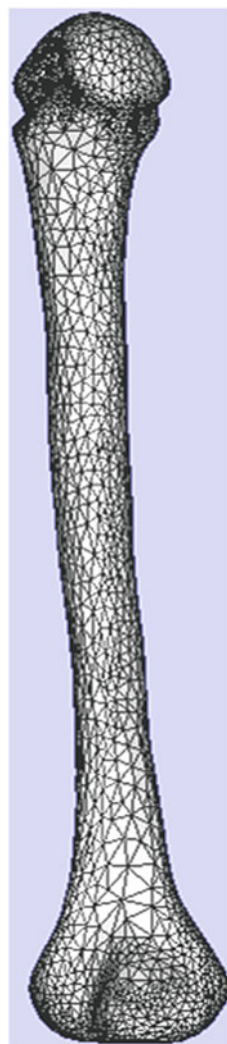
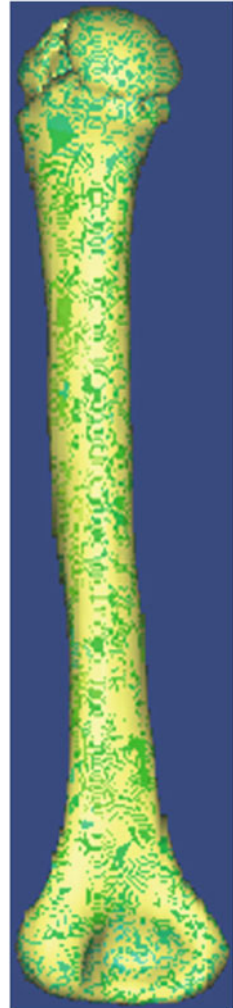


Fig. 4 Volumetric Mesh with material assignment



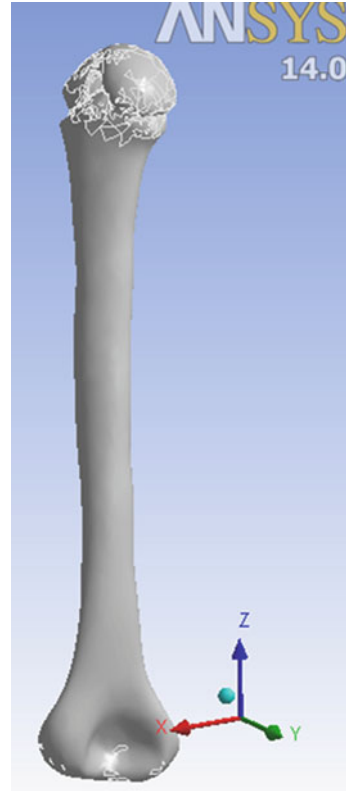
precision, the humongous task of MR spectroscopy. The slice thickness is 0.4 mm and resolutions are $1,024 \times 1,024$.

2. Procedure of establishing the model

(a) *Import the DICOM into MIMICS 10.01-*

All DICOM images are loaded and displayed and then by assigning a proper threshold value, based on Hounsfield Unit, the segmentation object is obtained, which is visualized by a colored mask containing only those pixels of images that we are interested in [16]. MIMICS 10.01 predefined a threshold of bone (CT), so we could easily select all bone tissue, the green

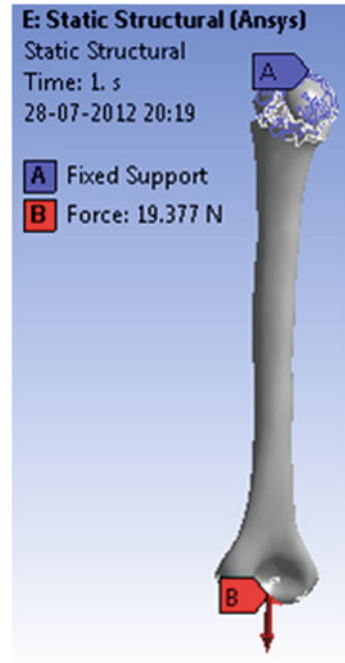
Fig. 5 3D Model for analysis



area was bone tissue pixels, we defined this as a mask. Based on the mask the humerus was selected, as in Fig. 2. This mask is modified until we get the satisfactory mask.

- (b) *Establishing FE model and generate surface mesh with MIMICS 10.01-* The generated region mask was used to develop 3D model for the bone. Based on 3D Grayvalue interpolation techniques 2D images are transformed into 3D model. It is a real 3D interpolation technique that takes into account the Partial Volume effect and therefore it is more accurate [16]. To obtain surface mesh, the option remeshing is used in order to raise the quality of the triangles so that the preprocessor of an FEA package can build a tetrahedron meshes from them (Fig. 3).
- (c) *Convert surface mesh into volumetric mesh with ABAQUS 6.10-* This mesh is exported to ABAQUS 6.10 and is converted from tri into tetra by using the mesh edit option. This is done because the denser the mesh the more realistic and more accurate will be the solution.

Fig. 6 Loading and boundary condition applied in ANSYS 14



(d) *Assign material properties in MIMICS 10.01-*

Materials are assigned to FEA meshes via the FEA menu or the FEA mesh tab. Before assigning materials to the elements of the volumetric mesh, Mimics will first calculate grayvalue for each element. After the calculation of the gray values of the elements of the volumetric mesh, the material assignment window will appear. We consider the default material properties of the CT data set. Using MIMICS STL+ module, humerus bone was converted into stereo lithography files for FE Analysis (Fig. 4).

3. Finite Element Analysis (FEA) using ANSYS 14

Elbow is one of the most complex joint in the human body and they are studied statically in a system [17]. Thus, the FEA mesh files are added in the FE modeler and then the model is transferred to static structural and further analysis is done under specific boundary and loading conditions (Fig. 5).

4. Loading and boundary condition

This biomechanical study was done based on some values calculated from some simulation studies done previously. The load was applied axially at the lower end of the humerus, in tension, keeping the humeral head fixed (Fig. 6).

Fig. 7 Maximum total deformation

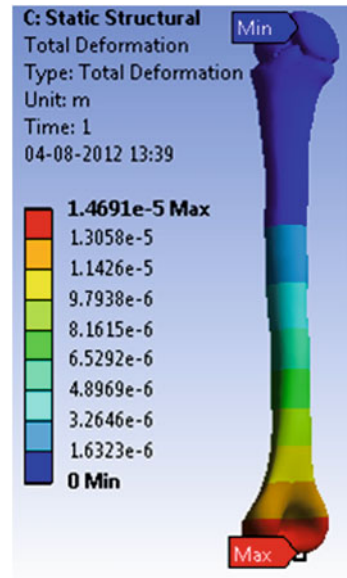
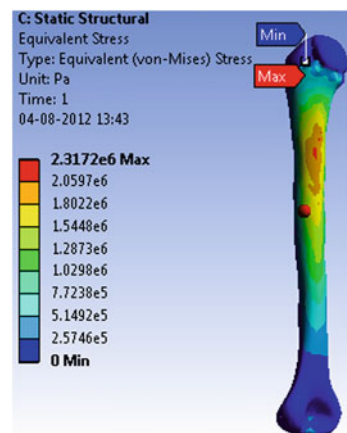


Fig. 8 Equivalent Von-Mises stress



Results and Discussions

Based on the analysis of the FE model, it was seen that the total deformation, equivalent stress, and strain increase with the increased load values. The fatigue safety factor for the bone is found to be appropriate considering the daily activities performed [18].

The purpose of our study was to establish a 3D FE model of humerus bones from volumetric CT data that will accurately capture the varying bone geometry and material properties. Arm bones are usually subjected to tensile forces during

Fig. 9 Elastic strain

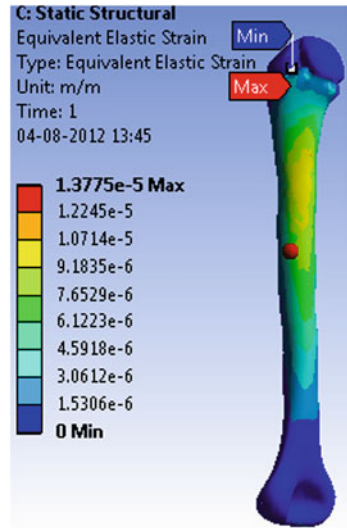
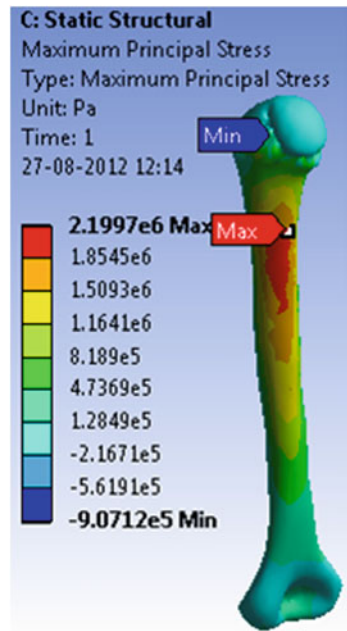


Fig. 10 Maximum principal stress



everyday weight lifting-related activities. In bending there is a combination of tensile and compressive force, tensile stress and strains on one side of the neutral axis and compressive stresses and strains on the other side [19]. By testing under tension, we cover the basic loading conditions to which the humerus bone can be subjected. The data collected from FEA showed the pattern of stress, strain, and

deformation of the bone at the interface that can be used to predict the failure of the bone material under load as shown in Figs. 7, 8, 9 and 10. This can help surgeons predict postoperative failures and analyze the cause of fractures taking place in the bone depending on the regions or zones where the maximum values of the stress, strain, and deformation exist.

S. No.	Parameters	$F = 707 \cdot \sin(7.8525 \cdot t)$	
		$t = 0.1$	$t = 0.2$
1.	Total deformation (mm)	0.0085356	0.014691
2.	Von-mises stress (MPa)	1.1636	2.3172
3.	Maximum principal stress (MPa)	1.1812	2.1997
4.	Elastic strain	5.8307e-6	1.3775e-5

Note Figures with results for Case $t = 0.2$ are shown in Figs. 7, 8, 9 and 10

Acknowledgments The authors thank Dr. Pushpraj Bhatele for providing medical imaging data. We also thank Dr. (Mrs.) Shobha Katheria, Principal Medical Officer, Ordnance Factory Hospital, Itarsi, M.P. India, for the back support, making us aware of the doctoral issues and practices. We are also thankful to all the faculty members of the Department of Mechanical Engineering, Government Engineering College, Jabalpur, M.P, India. Also, thanks to all study participants for their great effort and cooperation.

Conflict of Interest Statement None of the authors have any conflict of interest with the work described in this manuscript.

References

1. Toddes SP (2007) Optimization for commercialization of a two degree of freedom powered arm orthosis, Worcester Polytechnic Institute
2. Masih C, Francis A, Shriwastava A, Diwedi N, Tiwari P, Nareliya R, Kumar V (2012) Biomechanical evaluation of human humerus and scapula bone: a review. vol 3(1) Bioinfo Publications, India, pp 63–66, ISSN: 0976-8084 & E-ISSN: 0976-8092
3. Gray H (1821–1865) Anatomy of the human body-osteology-the humerus, 1918, <http://www.bartleby.com/107/51.html>
4. Kiran KC (2006) A study of surgical management of diaphyseal fractures of the humerus in adults by open reduction and internal fixation with dynamic compression plate and screws. Department of orthopedics. Kempegowda Institute of Medical Sciences, Bangalore
5. Alsamhan A, ELSingery MM, Zamzam MM, Darwish SM (2011) Engineering judgment of children bone fracture. Hindawi Publishing Corporation, Cairo, Vol 2011, Article ID 737054: 7
6. The skeleton: the arm and forearm. <http://home.comcast.net/~barbbranhm/arm.htm>
7. Nikander R (2009) Exercise loading and bone structure, studies in sports, physical education and health, University of Jyväskylä, ISBN 978-95131-3597-9
8. Nareliya R, Kumar V Biomechanical analysis of human femur bone. Int J Eng Sci Technol 3(4). ISSN: 0975-5462
9. Fung YC (1993) Biomechanics: mechanical properties of living tissues, 2nd edn. Springer, New York, p 511
10. Greene DA, Naughton GA (2006) Adaptive skeletal responses to mechanical loading during adolescence. Sports Med 36(9):723–732

11. Nieminen H, Niemi J, Takala EP, Juntura EV (1995) Load-sharing patterns in the shoulder during isometric flexion tasks. *J Biomech* 28:555–566
12. Einhorn TA (1992) Bone strength: the bottom line. *Calcif Tissue Int* 51:333–339
13. Turner CH, Burr DB (1993) Basic biomechanical measurements of bone: a tutorial. *Bone* 14:595–608
14. Bouxsein ML (2008) Technology inside: non invasive assessment of bone strength in osteoporosis. *Nat Clin Pract Rheumatol* 4:310–318
15. Gupta S, Dan P (2004) Trends biomaterial artificial organs, bone geometry and mechanical properties of the human scapula using computed tomography data 17(2):61–70
16. Materialise Interactive Medical Image Control System (MIMICS) (2011) 10.01: user guide
17. Lungu R, Borgazi E, Lungu M, Popa D, Tutunea D, Calbureanu MX (2010) New methods for the simulation with finite element of the human elbow. In: Proceedings of the international conference on circuits, systems, signals, pp 45–50
18. Westerhoff P, Graichen F, Bender A, Halder A, Beier A, Rohlmann A, Bergmann G (2009) In vivo measurement of shoulder joint loads during activities of daily living. *J Biomech* 42:1840–1849
19. Varghese BA (2011) Quantitative computed-tomography based bone-strength indicators for the identification of low bone-strength individuals in a clinical environment. Dissertation, Doctor of Philosophy, Wright State University